Recent Results from STAR

J.H. Thomas [a] for the STAR Collaboration

[a]Lawrence Berkeley National Laboratory
B510A, 1 Cyclotron Rd, Berkeley, CA 94720

Recent results from the STAR experiment are presented. The data indicate that nuclear matter produced in ultra-relativistic heavy ion collisions is hot, dense, and possibly opaque.

STAR is a wide aperature detector with full acceptance for hadronic observables out to $\approx 45°$ with respect to the beamline[1]. It is one of two large detectors at the Relativistic Heavy Ion Collider (RHIC) at Brookhaven National Laboratory. At the heart of STAR is the world's largest time projection chamber[2]; see figure 1. A silicon drift detector (SVT) surrounds the interaction vertex, and in the forward and backward directions there are radial drift TPCs (FTPCs) to cover the high rapidity region. Outside of the main TPC is a RICH detector and in the future STAR will be surrounded by a full barrel of electromagnetic calorimeters.

The data acquisition system is triggered by two independent signals: neutral energy measured in a pair of calorimeters at zero degrees with respect to the beam (Zcal) and by the multiplicity of particles that hit the central trigger barrel (CTB). The combination of the Zcal and CTB signals allow us to select events by centrality (or impact parameter).

STAR detected the first collisions at RHIC in June of 2000. Since then, we have made measurements during two very successful physics runs; Au on Au at $\sqrt{s} = 130$ GeV in 2000 and Au on Au at $\sqrt{s} = 19.6$ and 200 GeV in 2001-2002. We also ran polarized protons at 200 GeV in 2001-2002 but the proton data are beyond the scope of this brief report.

Typical spectra from the Au-Au runs cover ± 1 unit of rapidity. The measured momenta range from 150 MeV up to 1.0 GeV for identified particles in the TPC, up to 3 GeV for identified particles in the RICH, and out to 12 GeV for all charged particles.

STAR has collected a large sample of spectra for identified protons, pions, kaons (charged and neutral), and their anti-particles. And in the higher statistic runs we have spectra for lambdas, cascades, and omegas. A recently prepared set of anti-proton spectra at mid-rapidity are shown in figure 2.

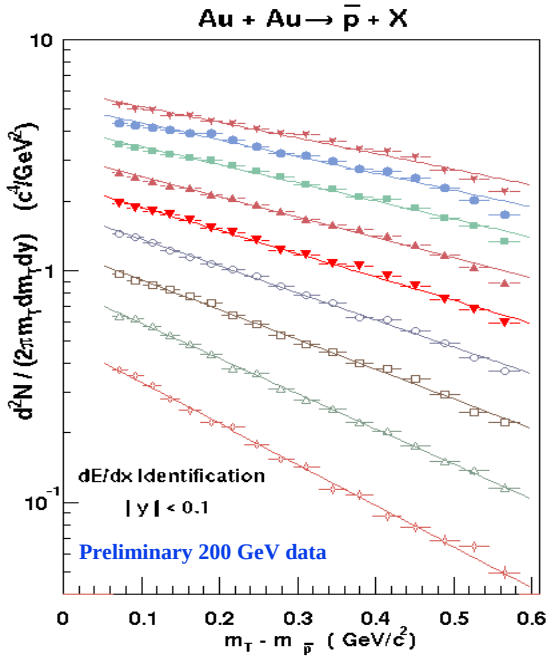

Figure 2. The multiplicity of anti-protons at $\sqrt{s}$ = 200 GeV are shown as a function of centrality. The lines are Gaussian fits to the spectra with respect to the transverse mass of the anti-protons. Each line represents a different centrality class.

The data are plotted as a function of centrality

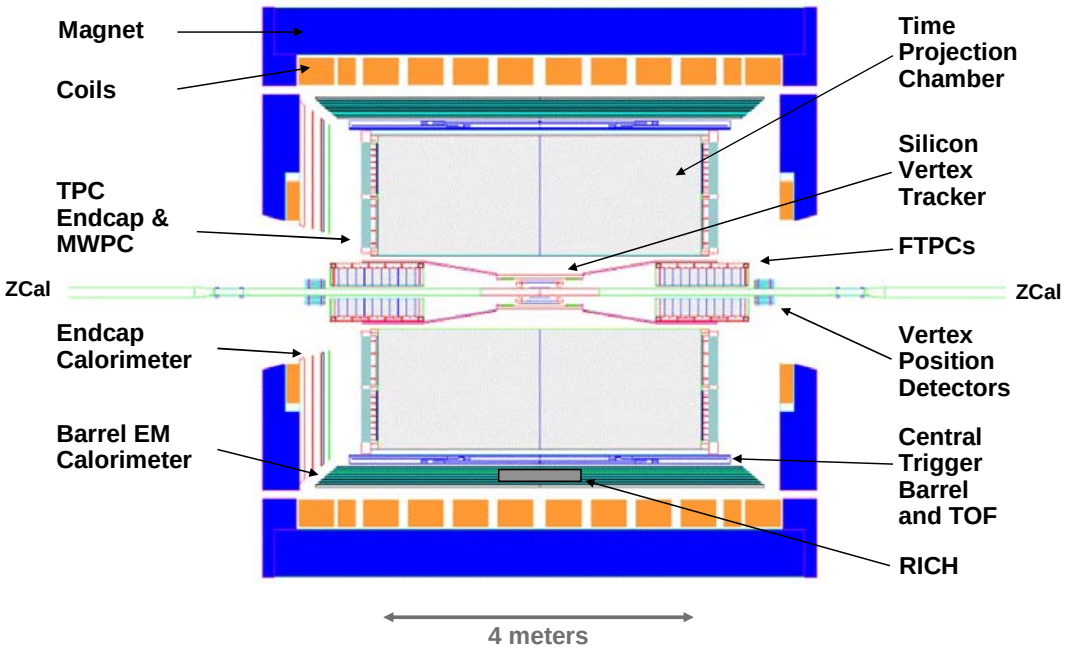

Figure 1. The STAR detector at RHIC. The full suite of detectors makes it possible to measure hadronic and leptonic observables over a wide rapidity interval and into 2π azimuth.

with the most peripheral collisions represented by the bottom curve on the plot and the most central collisions by the top-most curve. The top curve represents the top 5% of the cross-section for Au-Au interactions at 200 GeV, the next line represents the bin between 5 and 10% of the cross-section, and the bins are 10% wide after that. STAR has measured p and $\overline{\mathrm{p}}$ spectra at $\sqrt{\mathrm{s}}$ = 19.6, 130, and 200 GeV. The 19.6 and 200 GeV data are new, while the 130 GeV data are already in the literature[3].

The yield of anti-protons as a function of collision energy is interesting because there aren't any anti-baryons in the initial state at RHIC. Examination of the $\overline{\mathrm{p}}$/p ratio is one way to summarize the collision data. We have measured ratios of 0.11±0.01, 0.71±0.05, and 0.80±0.05 at 19.6, 130, and 200 GeV, respectively[4]. In the early Universe, we believe that the anti-baryon to baryon ratio was unity and so the data show a clear trend towards the early universe values for the $\overline{\mathrm{p}}$/p ratio as a function of $\sqrt{\mathrm{s}}$. Another way to appreciate this trend is to calculate the fraction of net baryons that are created by pair production. The observed $\overline{\mathrm{p}}$/p ratio suggests that 80% of the protons come from pair production and the remaining 20% are transported into the collision zone by the beam. So for the first time at a heavy ion collider, more baryons are pair produced than are present in the initial state.

The $\overline{\mathrm{p}}$/p ratio, and other particle ratios measured by STAR at 130 GeV, can be used as input to a simple model[5] to estimate the temperature of the system at the time of hadro-chemical freeze-out. The result is that T = 175 ± 7 MeV and μ_B = 51 ± 6 MeV. This temperature is not so different than what was seen at the SPS, however the baryo-chemical potential, μ_B, is much lower. ($\mu_B \cong$ 270 MeV at the SPS). Hadron resonance ideal gas models yield very similar results[6] but, perhaps, slightly lower chemical potentials $\mu_B \cong$ 40 MeV. It is interesting to note that these models assume thermal and chemical equilibrium at hadro-chemical freeze-out. The models also have predictive power and can accurately predict the particle ratios for species not

included in the input data.

Overall, the particle spectra at RHIC tell us where we are on the phase diagram of T .vs. μ_B. The chemical freeze-out temperature is high, 175 MeV, while the chemical potential is low, 40 MeV. The temperature is very close to the phase transition temperature predicted by lattice QCD, 173 MeV in a two flavor calculation[7], and it is unlikely that any hadronic system will achieve a higher temperature than this. So we know where we are on the phase diagram, but we don't know what other features are on the diagram . . . such as the location of the tri-critical point and whether the phase transition to the QGP is first order or second order and in a region accessible to RHIC. These are mysteries to be resolved in the future.

There is another freeze-out temperature in relativistic heavy ion collisions and it is the temperature of kinetic freeze-out. In elementary particle collisions, chemical and kinetic freeze-out occur at the same temperature; but in heavy ion collisions they occur at different temperatures. So if chemical freeze-out marks the end of inelastic collisions and the freezing of the number of chemical species, then kinetic freeze-out marks the end of elastic collisions and the freezing of particle momenta.

We can estimate the kinetic freeze-out temperature by studying the slopes and shapes of the particle spectra. The spectra in figure 2, for example, were plotted as a function of the transverse mass of the anti-proton and then fit with a Gaussian curve. You might expect the fundamental spectrum shape would be a Boltzman distribution or perhaps a Bose Einstein distribution (for pions or kaons). But a thermal distribution is not enough. These spectra are boosted by the hydrodyamical flow of the participants because heavy ion collisions generate pressure gradients inside the collision zone and these gradients drive a radial transverse expansion of the source. The symmetric expansion term is called radial flow.

Radial flow adds kinetic energy to the particle distribution and therefore modifies the spectrum shape. In figure 3, the effective temperature for the pions is 215 MeV, for the kaons it is 310 MeV, and for the anti-protons it is 575 MeV. The $< p_T >$ and the effective temperatures increase with mass. Thus, the classical expression for total energy

$$E_{tot} = \frac{3}{2}T + \frac{1}{2}mv^2 \quad (1)$$

suggests a linear relationship[8]

$$T_{obs} = T_{KFO} + mass \times \bar{\beta}^2 \quad (2)$$

where the observed temperature is the sum of a universal freeze-out temperature plus the addition of a kinetic energy term due to the high velocity of the expanding shock front.

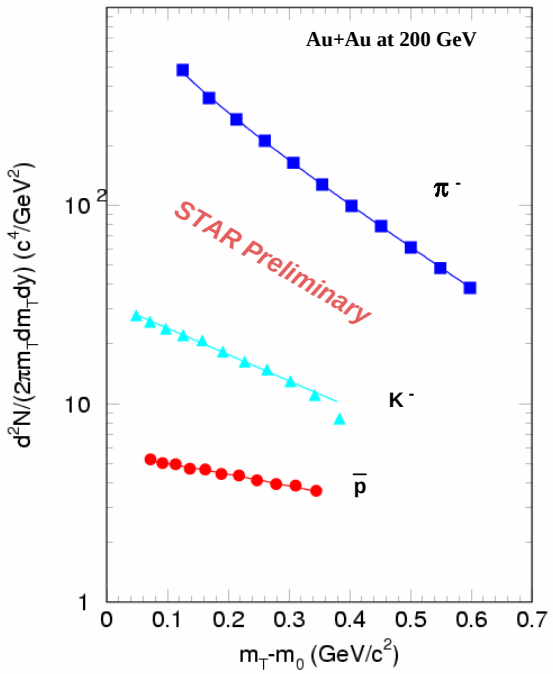

Figure 3. The slopes of the particle spectra decrease with mass, however the $< p_T >$ and the effective temperature increase with mass.

The freeze-out temperature for kinetic processes at RHIC is $\approx$ 100 MeV and this is approximately the same as the freeze-out temperature measured at the SPS; as a function of $\sqrt{s}$, freeze-out is constant from 10 GeV to 200 GeV. The mean expansion velocity is not constant, however. It increases with $\sqrt{s}$ and, at RHIC Energies, the mean radial expansion velocity is 60% of the speed of light.

There are other hydrodynamic effects in the data. Elliptic flow measures the anisotropic shape of the transverse flow field. It is the 2^{nd} harmonic Fourier coefficient of the momentum distribution of particles with respect to the reaction plane[9]. The ellipticity in spatial coordinates comes about because of the asymmetric overlap of two spheres in a non-central collision. However, a finite cross-section for re-interactions is required for this initial state spatial asymmetry to translate itself into a final state momentum space asymmetry; and the cross-sections must be large at early times or the details of the initial collision geometry could not manifest themselves in the final state momentum distributions.

We see elliptic flow in pion, kaon, proton, and lambda spectra. The amount of elliptic flow is large and in good agreement with hydrodynamic models for ultra-relativistic collisions. Even the mass dependence is well described by hydrodynamics[10]. This is interesting because hydro assumes local thermal equilibrium and large amounts of elliptic flow can only be generated if equilibrium is established very early in the time history of the collisions.

The surprising thing about our data is that elliptic flow persists to high momentum and then it saturates. The flow pattern shown in figure 4 follows the prediction of hydrodynamics up to about 2 GeV/c but hydro predicts that the flow curve should continue to rise above 2 GeV/c.

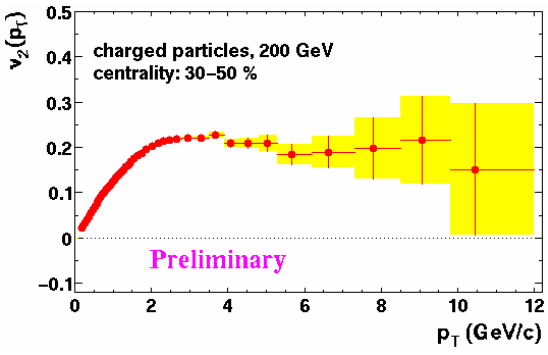

Figure 4. Elliptic flow is plotted as a function of p_T. The flow parameter, v_2, saturates at high p_T.

We observe that elliptic flow saturates at 2 GeV/c. Thus, there is some mechanism that builds pressure gradients, even at high p_T, and allows the asymmetry in the emission pattern to persist to the highest measured transverse momenta. This mechanism may be partonic energy loss or another exotic mechanism.

High transverse momentum spectra are interesting in other ways. For example, it is tempting to hypothesize that Au-Au collisions are a simple superposition of p-p collisions. We can test this hypothesis by comparing the normalized yield of charged particles for Au-Au collisions to those for p-p collisions as shown in figure 5. The normalization factor is taken to be the number of binary collisions in a Au-Au collision. Previous experience at the SPS has shown that soft collision processes scale as the number of participants while hard scattering processes scale as the number of binary collisions. Thus, neglecting shadowing and the Cronin effect, we expect the spectra to start from participant scaling at low p_T and evolve towards binary scaling at high p_T.

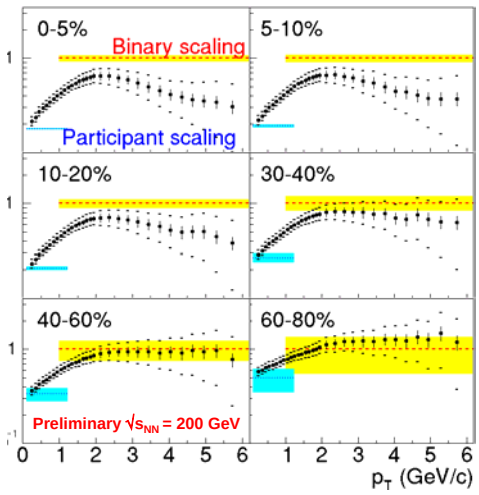

Figure 5. The normalized ratio of the Au-Au to the p-p yields for collisions at 200 GeV. Charged hadrons were measured in the range from 0 to 6 GeV/c. Systematic errors are indicated by the bars and the caps show the quadrature sum of the error bars with the systematic errors on the reference data.

The different panels in the figure show the ratio of cross-sections at different collision centralities.

We expect this ratio to be 1.0 at *high* p_T if a Au-Au collision is a trivial scaling of a p-p collision. So, for example, the *peripheral* collision data, in the lower right panel, show a smooth evolution from participant scaling at low p_T to binary scaling at high p_T. This is what we expect in a simple scaling hypothesis. But further examination of the data shows a clear violation of this hypothesis as the collisions become more and more central. The top left hand panel in figure 5 indicates that the ratio is suppressed by a factor of 3 in the most central collisions.

It isn't necessary to have a p-p reference spectrum in order to see the suppression of the high p_T spectra. The suppression can also be seen when the spectra are compared by centrality (ie. impact parameter). Figure 6 shows the ratio of central collisions to peripheral collisions at 130 and 200 GeV. The yields are normalized by the number of binary collisions expected in each centrality class.

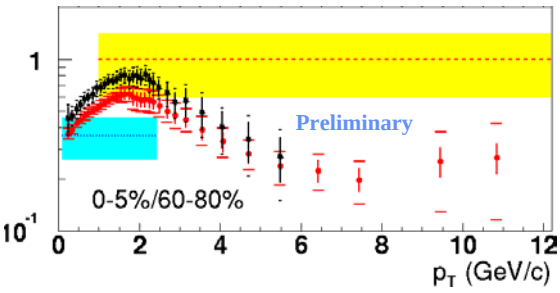

Figure 6. The normalized ratio of yields for central to peripheral Au-Au collisions at 130 and 200 GeV. The most central collisions (0-5%) are compared to the most peripheral collisions (60-80%). The 130 GeV data extend to 6 GeV and the 200 GeV data extend to 12 GeV.

The suppression of this ratio is especially interesting in view of the fact that the Cronin effect enhances the heavy ion cross-sections at high p_T and therefore the ratio should rise above one. We see the suppression effect in our 200 GeV data and in our 130 GeV data[11].

One possible explanation for the suppressed yield in central collisions is that there are new energy loss mechanisms that come into play at high p_T which distort the spectrum. A candidate mechanism is gluon bremmstrahlung. If a sufficiently dense medium exists in a heavy ion collision, then gluon bremsstrahlung and other dE/dx processes will shift particles out of the high p_T part of the spectrum and add them to the low p_T portion of the spectrum. Due to the exponential decrease in the cross-sections, a small shift out of the high p_T tail will look like a significant decrease in the ratio of yields in figures 5 and 6. This mechanism may also explain the persistence of elliptic flow at high p_T because the flow data require that primary particles interact with the expanding medium, even at high p_T.

The comparison of Au-Au collisions to p-p collisions is interesting in another way. How do jets in Au-Au collisions compare to jets in p-p collisions?

Jets are hard to find in heavy ion collisions because the high multiplicity of particles hides the jets, so we have done it using a statistical correlation technique. The correlation function is built by identifying a particle with a transverse momentum that exceeds a trigger threshold and then looking for associated high p_T particles at similar angles and rapidity intervals.

$$C_2(\Delta\phi, \Delta\eta) = \frac{1}{N_{trigger}} \frac{N(\Delta\phi, \Delta\eta)}{Efficiency} \qquad (3)$$

The correlation data show that jets exist in central collisions at RHIC and we have previously reported on them at 130 GeV[12]. However, other correlations exist in heavy ion collisions which may not exist in p-p collisions. Elliptic flow is an example. So, we need a technique to distinguish one correlation from the other.

We have done this by looking in the non-jet region ($45° < \Delta\phi < 125°$) and building up the correlation function in and out of the jet cone. The new correlation function is shown below:

$$C_2(Au+Au) = C_2(p+p) + A^*(1 + 2v_2^2 \cos(2\Delta\phi)) \qquad (4)$$

It includes the p-p correlation and the effects of elliptic flow. The v_2 parameter was determined independently by a reaction plane analysis and

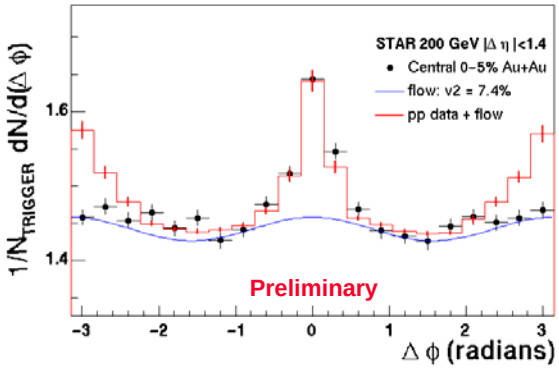

Figure 7. The observed jet like correlation function in heavy ion collisions is compared to the correlations seen in p-p collisions. The effects of elliptic flow are added to the p-p reference function. Note that the correlation is suppressed at 180 degrees in Au-Au.

the magnitude, A*, of the flow term was fit in the non-jet cone region. The fit is shown in figure 7.

The correlation functions for Au-Au and p − p(+flow) collisions are very similar in the forward jet cone region ($|\Delta\phi| < 1$ radian). But the correlation functions are different in the backward cone region and, in particular, the backward going jets in Au-Au are suppressed. What does this mean? It may mean that a jet can only be seen in a heavy ion collision when it originates near the surface of the collision zone. The backward going jet is suppressed; either because the fireball is opaque to high p_T particles, or, perhaps, the angular correlation with the away side jet is destroyed by multiple gluon exchange in the gluon saturated core of the fireball.

Conclusions

Nuclear matter created by collisions of heavy ions is not a trivial convolution of nuclear matter created by collisions of protons. Our analyses at 130 and 200 GeV show that the fireball created in RHIC collisions is very dense and possibly opaque. Novel and new energy loss mechanisms will be required to explain how high p_T particles interact with this hot and dense matter.

Our data show that nuclear matter produced in RHIC collisions is accurately described by hydrodynamic models which assume local thermodyamic equlibrium at very early times in the collision sequence. And we have achieved the highest temperature possible for chemical freeze-out. A higher freeze-out temperatures cannot be achieved in heavy ion collisions.

The properties of the material produced in these collisions lie in an entirely new region of the phase diagram for nuclear matter and it lies at the boundary between hadronic matter and the quark gluon plasma.

In summary, nuclear matter at RHIC is hot, it is dense, it's expanding rapidly, and its properties are not inconsistent with local thermal equilibrium.

REFERENCES

1. The STAR Collaboration homepage is located at http://www.star.bnl.gov. Our journal contributions can be found by clicking on "Publications".
2. H.H. Wieman *et al.*, IEEE Trans. Nuc. Sci. **44**, 671 (1997) and J.H. Thomas *et al.*, Nucl. Instrum & Meth. **A478**, 166 (2002).
3. C. Adler *et al.*, Phys. Rev. Lett. **87**, 262302-1 (2001).
4. We previously reported the $\overline{p}$/p ratio to be 0.60±0.06 at 130 GeV. This analysis was based on a limited data sample and a more extensive dataset is now available.
5. Braun-Munzinger *et al.*, Phys. Lett. **B518**, 41-46 (2001) and hep-ph/105229.
6. N. Xu and M. Kaneta, Nucl. Phys. **A698** , 306-313 (2002) and nucl-ex/0104021.
7. F. Karsch, Nucl. Phys. **A698**, 199 (2002) and hep-lat/0106019, hep-ph/0103314.
8. N. Xu, Nucl. Phys. **A610**, 175c (1996).
9. K.H. Ackermann *et al.*, Phys. Rev. Lett. **86,** 402-407 (2001).
10. C. Adler *et al.*, Phys. Rev. Lett. **87**, 182301 (2001).
11. C. Adler *et al.*, nucl-ex/0206011.
12. C. Adler *et al.*, submitted to Phys. Rev. Lett. and nucl-ex/0206006.